A Quasi-Linear, Viscoelastic, Structural Model of the Plantar Soft Tissue With Frequency-Sensitive Damping Properties

William R. Ledoux[1]
e-mail: wrledoux@u.washington.edu
Ph.D., Department of Veterans Affairs, RR&D Center of Excellence for Limb Loss Prevention and Prosthetic Engineering, VA Puget Sound Health Care System, Seattle WA, 98108, and, Department of Mechanical Engineering and Department of Orthopaedics and Sports Medicine, University of Washington, Seattle, WA, 98195

David F. Meaney
Ph.D., Department of Bioengineering, University of Pennsylvania, Philadelphia, PA 19104

Howard J. Hillstrom
Ph.D., Gait Study Center, Temple University School of Medicine, Philadelphia, PA 19107

Little is known about the structural properties of plantar soft-tissue areas other than the heel; nor is it known whether the structural properties vary depending on location. Furthermore, although the quasi-linear viscoelastic (QLV) theory has been used to model many soft-tissue types, it has not been employed to model the plantar soft tissue. The structural properties of the plantar soft tissue were quantified via stress relaxation experiments at seven regions (subcalcaneal, five submetatarsal, and subhallucal) across eight cadaveric feet. The cadaveric feet were 36.9±17.4 (mean±S.D.) years of age, all free from vascular diseases and orthopedics disorders. All tests were performed at a constant environmental temperature of 35°C. Stress relaxation experiments were performed; different loads were employed for different areas based on normative gait data. A modification of the relaxation spectrum employed within the QLV theory allowed for the inclusion of frequency-sensitive relaxation properties in addition to nonlinear elastic behavior. The tissue demonstrated frequency-dependent damping properties that made the QLV theory ill suited to model the relaxation. There was a significant difference between the elastic structural properties (A) of the subcalcaneal tissue and all other areas ($p=0.004$), and a trend ($p=0.067$) for the fifth submetatarsal to have less viscous damping (c_1) than the subhallucal, or first, second, or third submetatarsal areas. Thus, the data demonstrate that the structural properties of the foot can vary across regions, but careful consideration must be given to the applied loads and the manner in which the loads were applied.
[DOI: 10.1115/1.1824133]

Keywords: Foot, Biomechanics, Heel, Metatarsals

Introduction

During the stance phase of walking, load is transmitted from the lower extremity to the ground through the plantar soft tissue. There are seven primary regions through which force is typically applied, namely the tissue beneath the heel (subcalcaneal), the five metatarsal heads (submetatarsal), and the big toe or hallux (subhallucal) [1]. The cross-sectional anatomy of all areas is similar, as each has skin and a layer of adipose tissue retained by elastic septa. The areas other than the subcalcaneal area may also have tendons and tendon insertions [2].

The previously reported mechanical testing of the plantar soft tissue has concentrated on the subcalcaneal region, with either in vivo instrumented impact tests [3–5] or in vitro material testing machine experiments [6]. The in vitro tests resulted in less percent energy absorption (29% to 32% versus 73% to 85%), less deformation (2.1 to 4.7 mm versus 8.5 to 11.3 mm) and increased stiffness (1.16×10^6 N/m versus 1.0×10^5 to 1.75×10^5 N/m) than the in vivo tests. Aerts et al. performed modified testing protocols to ensure similar experimental conditions for the instrumented impact tests and materials testing experiments. They measured similar values of stiffness ($\sim9.0\times10^5$ N/m), displacement (~5 mm), and energy loss (46.5%–65.5%) for both tests, suggesting that the presence of the entire lower leg affects the in vivo results [7]. However, four of the five feet tested were older than 50 years of age with peripheral vascular disease (PVD) and the experiments were all done at room temperature, factors which could potentially affect the soft-tissue properties [5,8–12]. Recently, a study by Miller-Young et al. has examined the material properties of the subcalcaneal tissue; however, the investigators used older specimens, tested at room temperature, and made no mention of the vascular state of the tissue [13].

The primary goal of this research was to quantify the structural properties of the plantar soft tissue at seven regions of interest. We extended previous studies by investigating specific subregions of the plantar soft tissue that experience mechanical loading during gait. In order to simulate in vivo conditions with young, healthy specimens, we excluded older or diabetic subjects and controlled the temperature of the specimens during testing. To more accurately model the measured structural properties, we employed a modified form of the quasi-linear viscoelastic (QLV) theory to account for frequency-sensitive damping properties.

Methods

Eight fresh frozen (less than 24 h postmortem) cadaveric feet (three male and five female) were radiographed for gross orthopedic irregularities. The feet were relatively young—36.9±17.4 years (mean±S.D.), range 18 to 58 years, and free of PVD. The feet came from specimens with a body weight (BW) of 757±297 N (mean±S.D.). Each foot was mounted plantar side superiorly in polymethylmethacrylate (PMMA) in an aluminum box. The initial, unloaded tissue thickness for each of the seven areas was calculated by placing small metallic washers on the areas of interest, inserting needles of known lengths through the washers until they reached bone, and then x raying the specimens. The initial thickness was defined as the distance between the washer and the tip of the needle.

The seven areas on each foot (subcalcaneal, five submetatarsal, and subhallucal) were tested with an IRB-approved protocol on an Instron series 1331 materials testing machine (Instron Corporation; Canton, MA) with a 1780 N load cell (±0.2 N) (Fig. 1). The initial, unloaded thickness of the tissue was registered to the loading frame by lowering the crosshead until the circular cross-section punch just touched the tissue (as determined via visual inspection). The diameters of the punches (2.54 cm for the subhallucal and first metatarsal areas, 1.27 cm for the lesser submetatarsal areas, and 4.06 cm for the subcalcaneal region) were based on osseous geometry [2,14]. The specimens were heated to slightly less than core body temperature (35°C instead of 37°C since extremities are usually cooler) using a closed-loop temperature control system with a thermocouple placed between the foot and the PMMA. The foot, aluminum box, and punch were surrounded with foam insulation and the skin temperature of the foot was monitored independently.

The physiologic target loading levels simulating gait for each region were calculated from the specimen BW (obtained with the

[1]To whom correspondence should be addressed.

Contributed by the Bioengineering Division for publication in the JOURNAL OF BIOMECHANICAL ENGINEERING. Manuscript received by the Bioengineering Division March 7, 2003; revision received July 2, 2004. Associate Editor: Philip V. Bayly.

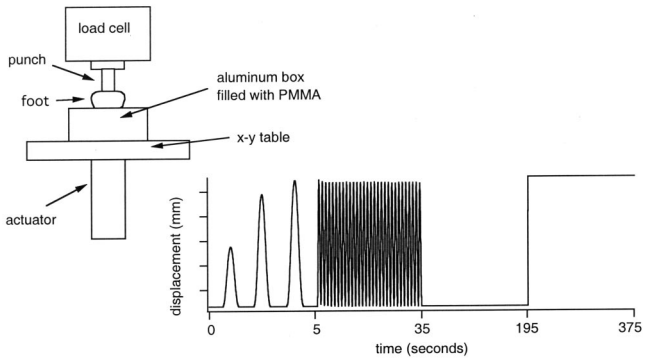

Fig. 1 A schematic of the testing apparatus and the mechanical input data input. In the schematic, the foot is viewed posteriorly. Note that the dorsal surface of the foot is placed into the PMMA. The graph is the input displacement for the experiment, including the haversines of increasing amplitude (0 to 5 s), the preconditioning (5 to 35 s), the delay period (35 to 195 s), and the ramp and hold (195 s to 375 s). Note that the *x* axis was not drawn proportionally.

donor information) and the peak force in BW during stance phase for each region (Table 1) [15]. Successive 1-Hz displacement control haversines of increasing amplitude were applied to each specimen until the desired physiologic target load was achieved. This target displacement was then used for all subsequent tests.

The tissue was preconditioned with 1-Hz haversines to the target displacement for 30 s. Before the next test, the machine had to be manually reconfigured for a stress relaxation protocol. To ensure proper and consistent reconfiguration for all experiments, a time delay of 3 min was implemented after the preconditioning phase and before the relaxation test. A ramp and hold displacement function was then applied with a ramp time of approximately 0.3 s and a relaxation period of 175 s (enough time for the specimens to reach steady state) (Fig. 1). Data were sampled at 100 Hz during the displacement pulses and preconditioning, and at 250 Hz for the ramp and hold.

The quasi-linear viscoelastic (QLV) theory has been employed to model the behavior of various biological tissues [16–21]. The theory, which assumes that the spatial characteristics [i.e., the elastic response, $F^{(e)}(\varepsilon)$] and the temporal characteristics [i.e., the reduced relaxation response, $G(t)$] are independent, is described with the following equation:

$$F(t)=\int_0^t G(t-\tau')\frac{\partial F^{(e)}[\varepsilon(\tau')]}{\partial\varepsilon}\frac{\partial\varepsilon(\tau')}{\partial\tau'}d\tau' \tag{1}$$

where F is the force and ε is the strain. Note that the model is structural; therefore, we are reporting force. However, since we were able to determine the initial soft-tissue thickness, the displacement was reported as strain. Force and strain have been used together previously [21].

Table 1 The target force in body weight (BW) [15] and Newtons (N), based on the average BW (757 N) of the cadaveric specimens in the this study

Region	Target force (BW)	Target force (N)
Subcalcaneal	0.944	714.1
First submetatarsal	0.185	140.0
Second submetatarsal	0.131	99.1
Third submetatarsal	0.097	73.4
Fourth submetatarsal	0.067	50.7
Fifth submetatarsal	0.040	30.3
Subhallucal	0.218	164.9

The normalized compression (c), substituted for the strain in Eq. (1), is defined as the displacement (δ) from the point where the compressive force began to monotonically increase during the stress relaxation test

$$c=\delta/b \tag{2}$$

where the thickness (b) is the tissue thickness at the point when the force began to monotonically increase. This accounted for any slackness in the system without artificially inflating the strain.

The following elastic function is employed [17]:

$$F^{(e)}(c)=A(e^{Bc}-1) \tag{3}$$

where A and B are the elastic constants, F is the force, and c is the normalized compression. The form of the reduced relaxation response is as follows [16]:

$$G(t)=\frac{1+\int_0^\infty S(\tau)e^{-t/\tau}d\tau}{1+\int_0^\infty S(\tau)d\tau} \tag{4}$$

where $S(\tau)$ represented the relaxation spectrum. Iatridis et al. developed a frequency-sensitive relaxation spectrum [20], which is defined as

$$S(\tau)=\begin{cases}\dfrac{c_1}{\tau}+\dfrac{c_2}{\tau^2} & \text{for } \tau_1\leqslant\tau\leqslant\tau_2\\ 0 & \text{for } \tau<\tau_1,\ \tau>\tau_2\end{cases} \tag{5}$$

where c_1 is the amplitude of the viscous effects, c_2 is the linear increase in viscous effects with frequency, while τ_1 and τ_2 represent the time values corresponding to the frequency limits of the relaxation spectrum.

The normalized compression was described as a function of time for substitution into Eqs. (2) and (3). Since the ramp was not ideal, two linear fits were employed, where the slope (strain rate) was $\dot{c}_s$ for $0\leqslant t\leqslant t_s$ and $\dot{c}_o$ for $t_s<t\leqslant t_0$, with t_0 being the ramp time. The full form of the QLV theory employed in this study was obtained by substituting Eqs. (3), (4), and (5) into Eq. (1) (see the Appendix).

The analytical representation of $F(t)$ at $t>t_0$ [Eq. (*A*7)] was normalized by $F(t_0)$ and used to fit the relaxation data. The value for τ_2 was assumed to be the last point in time of the experimental data. The nonlinear elasticity constant (B) and relaxation spectrum parameters (c_1, c_2 and τ_1) were obtained by curve fitting the data at $t>t_0$ normalized to the peak force with a Levenberg–Marquardt nonlinear least-squares algorithm (Igor Pro, WaveMetrics, Inc.; Lake Oswego, OR). The elastic constant (A) was obtained, in newtons (N) and body weight (BW), by substituting the solved coefficients into the equation for $F(t)$ [Eq. (*A*7)] and curve fitting the unnormalized data.

For qualitative comparison, the relaxation data from each area were averaged together. For quantitative analysis, each *individual* trial was curve fit using the modified QLV theory. An analysis of variance (ANOVA) was performed to determine if there were significant differences ($\alpha=0.05$) between coefficients from different locations of the plantar soft tissue; Fisher's protected least significant difference was used for posthoc analysis. Representative curves for each region were generated from the average coefficients of each location.

Results

Due to either mechanical problems (incorrect ramp rate [$n=1$], over ranged displacement [$n=3$], incorrect initial position of crosshead [$n=2$], early termination of data acquisition

Table 2 The structural testing conditions, including the number of specimens, the soft-tissue thickness, the average peak strain and the two strain rates ($\dot{c}_s$ and $\dot{c}_o$), the ramp times for the bilinear strain curve (t_s and t_o), the average peak force, and percent difference from the target force

Region	Number of specimens	Avg. thick. (±S.D.) (mm)	Avg. peak strain (±S.D.) (mm/mm)	Avg. $\dot{c}_s$ (1/s)	Avg. $\dot{c}_o$ (1/s)	Avg. t_s (s)	Avg. t_o (s)	Avg. peak force (±S.D.) (N)	Difference from target (%)
Subcalcaneal	6	17.10±3.63	0.439±0.073	2.015	0.354	0.203	0.344	644.6±384.3	9.74
First submetatarsal	7	10.65±1.47	0.510±0.108	2.731	0.522	0.165	0.288	136.2±58.9	2.65
Second submetatarsal	7	16.56±1.76	0.497±0.108	2.732	0.475	0.163	0.286	83.9±43.4	15.31
Third submetatarsal	6	15.57±2.14	0.489±0.111	2.920	0.561	0.144	0.260	64.0±29.1	12.78
Fourth submetatarsal	6	15.03±1.49	0.501±0.152	2.696	0.532	0.162	0.288	51.7±23.5	−2.06
Fifth submetatarsal	4	12.84±1.06	0.520±0.113	2.802	0.588	0.165	0.296	31.3±10.1	−3.46
Subhallucal	8	8.66±1.70	0.429±0.184	2.469	0.535	0.157	0.264	164.5±61.8	0.26

$[n=1]$, or poor signal to noise ratio $[n=1]$) or thermal problems (specimen not heated $[n=1]$ or temperature drift due to improper insulation $[n=4]$), data from 13 of the plantar soft tissue regions were discarded. The data from the remaining trials are summarized in Table 2. The thickness and peak strain correspond to physiological values [22,23] and the peak force generated was within 15% of the target force for all seven areas.

The characteristic nonlinear relaxation semi-log plot (i.e., the slope is not uniform, but rather the data exhibit frequency-sensitive damping, meaning that the short-term, or high-frequency, relaxation is faster than the long-term, or low-frequency, relaxation) was seen for the average data from all seven regions (Fig. 2).

The only significant differences for the QLV coefficients between areas was for the elastic constant A (Table 3), with the subcalcaneal region being larger than all other areas for both the unnormalized and BW normalized curves ($p=0.004$ and $p<0.0001$, respectively). There was borderline significant difference for c_1 ($p=0.067$), with the fifth submetatarsal trending to have lower values than the subhallucal as well as the first, second, and third submetatarsal areas. No other significant differences were found with the number of specimens available in our sample.

For both the normalized and unnormalized data, the representative curves generated from the average coefficients of each location were for the most part within 1 standard deviation of the average relaxation curve (Figs. 2 and 3). The unnormalized curves were in general more variable than the normalized curves.

Discussion

Stress relaxation experiments were conducted on seven regions of eight cadaveric specimens; potential confounding factors, such as temperature, age, or presence of peripheral vascular disease, were controlled. A modified form of the QLV that included frequency-sensitive damping was developed and employed. The QLV model, as developed by Fung [16], assumes that the amplitude of the viscous effects are constant over a range of frequencies [20], which results in uniform slope when the relaxation data are graphed on a semi-log plot. Our relaxation data, however, demonstrated that the amplitude of the viscous effects varied with frequency [20]. This resulted in a stress relaxation curve with a slope that varied with frequency. Thus, the form of the QLV that Fung described did not adequately model our data and we had to develop a modified form of the QLV based on Iatridis et al.'s work.

The limitations of this study included the use of fresh frozen cadaveric tissue rather than live specimens. However, Bennett and Ker have demonstrated that heel pads tested immediately after amputation yielded results that were ''indistinguishable'' from data obtained from heel pads that were frozen, thawed, and tested [6]. It should also be noted that, like most previously published mechanical tests on the plantar soft tissue, except for notably Miller-Young et al. [13], the tests performed here were structural in nature. Thus, the results are only representative of these particular feet in the testing apparatus we employed. Another limitation was that position of the initial position of the punch was determined via visual inspection. However, we could not use a threshold force to set the initial position because the initial thickness was determined via x rays, needles, and washers in a manner such that no force except the weight of the washer was applied to the foot. The requirement that the nonlinear elastic coefficients be determined by the relaxation data was an additional limiting factor. Another possible concern was that the controller of the materials testing machine precluded testing the tissue immediately after the preconditioning; thus, we implemented a 3 min hold that unavoidably allowed for partial recovery of the tissue. However, the same delay was used for every test; thus, the results are comparable. A further limitation is that the time of the ramp phase (t_0) of the relaxation protocol was longer than the initial boundary of the relaxation spectrum (τ_1). As a result, it is most likely that some relaxation had occurred before the ramp reached maximum deformation. A survey of past research with the QLV demonstrated that a majority of users have ramp times longer than the first boundary of the relaxation specimen [18,19,24,25]; only one accounted for the relaxation [18]. Other researchers reported short ramp times but, in both instances, the authors were testing specimens with very small applied loads, allowing for the rapid movement of their materials testing machines [20,26]. Larger forces, as in this study, typically resulted in larger ramp times. Finally, by setting the final boundary of the relaxation spectrum (τ_2) equal to the test duration, we assumed that the tissue had fully relaxed by this time. If the tissue were still relaxing, then we would have underestimated τ_2.

The classic form of the QLV theory did not completely model the plantar soft tissue because of the assumption of frequency insensitivity required with Fung's theory [16]. Iatridis et al.'s modification of the QLV theory allowed for frequency-sensitive behavior to be accounted for in the constitutive model [20]. Iatridis et al.'s modifications, however, incorporated a linear elastic response while the plantar soft tissue was nonlinear. In the current work, a further modification was performed by incorporating both the nonlinear elastic function [17] and the frequency-sensitive reduced relaxation function [20], resulting in a nonlinear, frequency-sensitive constitutive relationship.

Direct comparison to other papers that have studied the mechanical properties of the plantar soft tissue is difficult since most of the literature deals with force versus deformation data [3–6]. The results from these studies, such as energy loss and stiffness, are not comparable to our work. Other groups have used ultrasound probes to develop elastic models of the soft tissue [27,28], but the models are very different from our work. The only paper that we are aware of that presents relaxation data for the plantar soft tissue is the work of Miller-Young [13]. However, theirs was a *material* study, while ours was *structural* in nature.

These data show that the structural properties of the plantar soft tissue can vary across the foot surface and that a modified form of the QLV theory was able to model the tissue response. A next step is to determine if these differences are material or structural in nature. Further, we will incorporate these distinct structural prop-

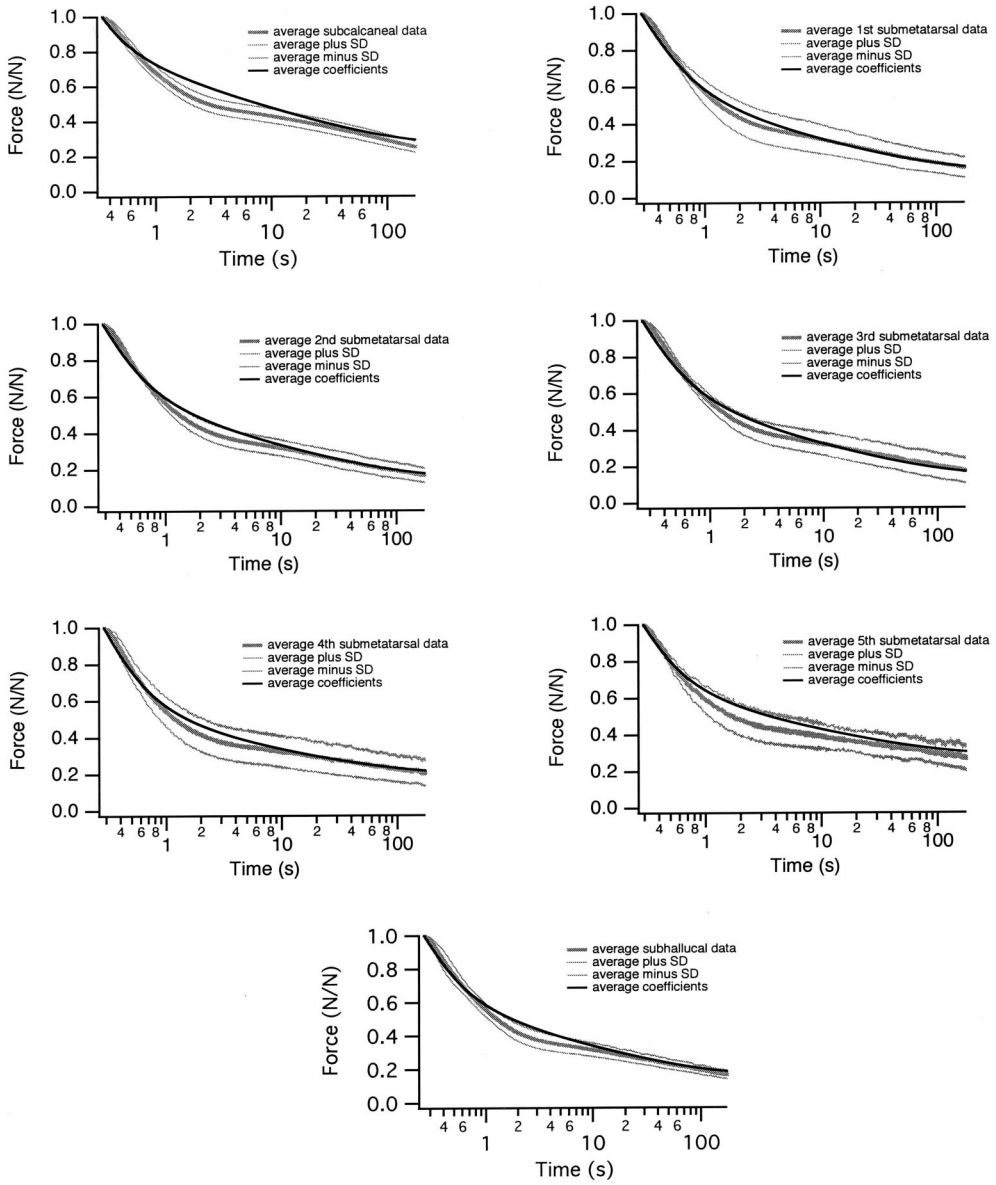

Fig. 2 The average stress relaxation (normalized force vs time) data (±1 S.D.) and the fit generated from the average QLV coefficients for the subcalcaneal, five submetarsal, and subhallucal areas

erties in a model of the foot during gait to determine how these spatial properties influence distribution of forces across the foot surface.

Acknowledgments

This research was partially supported by the Ashton Fellowship from the University of Pennsylvania, and by an internal grant from the Temple University School of Podiatric Medicine.

Nomenclature

A = elastic constant
B = elastic constant
b = tissue thickness
c = normalized compression
$\dot{c}_s$ = slope of normalized compression for $0 \leqslant t \leqslant t_s$
$\dot{c}_o$ = slope of normalized compression for $t_s < t \leqslant t_0$
c_1 = amplitude of the viscous effects
c_2 = linear increase in viscous effects with frequency
$E_1(z)$ = exponential integral
$F(t)$ = force
$F^{(e)}(\varepsilon)$ = elastic response of the QLV theory
$G(t)$ = reduced relaxation response of the QLV theory
R_i = substitution term, where $i = 1$ to 5
S_i = substitution term, where $i = 1$ to 10
$S(\tau)$ = relaxation spectrum
t = time
$\underline{t}$ = substitution time term
$\hat{t}$ = substitution time term
T_i = substitution term, where $i = 1$ to 12
t_s = time point where slope of normalized compression changes
t_0 = time point where maximum normalized compression is reached
δ = displacement
ε = strain
$\dot{\varepsilon}_s$ = strain rate for $0 \leqslant t \leqslant t_s$
$\dot{\varepsilon}_o$ = strain rate for $t_s < t \leqslant t_0$

Table 3 The QLV parameters (mean±S.D.) for each region

Region	A (N)	A (BW)	B (mm/mm)	c_1 (s)	c_2 (s^2)	τ_1 (s)
Subcalcaneal	485.2±520.5	0.607±0.409	2.37±0.976	0.314±0.067	0.165±0.121	0.089±0.044
First submetatarsal	66.2±51.3	0.103±0.030	2.05±0.404	0.438±0.130	0.703±0.476	0.144±0.040
Second submetatarsal	69.2±57.7	0.084±0.042	1.87±0.477	0.434±0.193	0.586±0.460	0.127±0.036
Third submetatarsal	52.9±25.6	0.064±0.021	1.90±0.558	0.440±0.261	0.579±0.497	0.122±0.051
Fourth submetatarsal	42.6±18.7	0.055±0.032	1.78±0.516	0.252±0.129	0.532±0.346	0.126±0.020
Fifth submetatarsal	36.3±31.8	0.036±0.022	1.52±0.605	0.188±0.113	0.279±0.136	0.113±0.031
Subhallucal	118.6±46.6	0.163±0.053	2.44±0.846	0.408±0.118	0.482±0.288	0.114±0.049
p-value	0.004	<0.0001	0.2	0.067	0.2	0.4
Posthocs	Subcalc>all	Subcalc>all		Fifth submet< first, second, and third submets, and subhall		

τ = time
τ' = time
τ_1 = lower frequency limit of the relaxation spectrum
τ_2 = upper frequency limit of the relaxation spectrum

Appendix

The elastic and reduced relaxation functions suggested by Fung [Eqs. (3) and (4)] and the relaxation spectrum offered by Iatridis et al. [Eq. (5)] were substituted into the general form of the QLV [Eq. (1)] and integrated. [Note that the general expression for strain (ε) was used, rather than normalized compression (c)]. This resulted in the following expression for the first part of the ramp ($0 \leq t \leq t_s$):

$$F(t) = R_1\left(R_2(t) + \frac{c_1}{B\dot{\varepsilon}_s}[R_3(t) + e^{B\dot{\varepsilon}_s t}\{R_4(t)\}] + c_2 e^{B\dot{\varepsilon}_s t}[R_5(t)] \right) \tag{A1}$$

$$R_1 = \frac{AB\dot{\varepsilon}_s}{1 + c_1 \ln\frac{\tau_2}{\tau_1} + c_2\left(\frac{1}{\tau_1} - \frac{1}{\tau_2}\right)} \tag{A2a}$$

$$R_2(t) = \frac{e^{B\dot{\varepsilon}_s t} - 1}{B\dot{\varepsilon}_s} \tag{A2b}$$

$$R_3(t) = E_1\left(\frac{t}{\tau_1}\right) - E_1\left(\frac{t}{\tau_2}\right) \tag{A2c}$$

$$R_4(t) = \ln\left(\frac{1 + B\dot{\varepsilon}_s\tau_2}{1 + B\dot{\varepsilon}_s\tau_1}\right) + E_1\left(\frac{t(1 + B\dot{\varepsilon}_s\tau_2)}{\tau_2}\right) - E_1\left(\frac{t(1 + B\dot{\varepsilon}_s\tau_1)}{\tau_1}\right) \tag{A2d}$$

$$R_5(t) = \ln\left(\frac{\tau_2(1 + B\dot{\varepsilon}_s\tau_1)}{\tau_1(1 + B\dot{\varepsilon}_s\tau_2)}\right) + E_1\left(\frac{t(1 + B\dot{\varepsilon}_s\tau_1)}{\tau_1}\right) - E_1\left(\frac{t(1 + B\dot{\varepsilon}_s\tau_2)}{\tau_2}\right) \tag{A2e}$$

where E_1 is defined as exponential integral: [29]

$$E_1(z) = \int_z^\infty \frac{e^{-t}}{t}\,dt \tag{A3}$$

The equation for the second portion of the ramp ($t_s < t \leq t_0$) was

$$F(t) = S_1\left(S_2(t) + \frac{c_1}{B}[S_3(t) + S_4(t) + S_5(t) + S_6(t) + S_7(t)] + c_2\dot{\varepsilon}_s e^{B\dot{\varepsilon}_s t}[S_8(t) + S_9(t)] + c_2 e^{B\dot{\varepsilon}_o t}[S_{10}(t)] \right) \tag{A4}$$

$$S_1 = \frac{AB}{1 + c_1 \ln\frac{\tau_2}{\tau_1} + c_2\left(\frac{1}{\tau_1} - \frac{1}{\tau_2}\right)} \tag{A5a}$$

$$S_2(t) = \frac{e^{B\dot{\varepsilon}_s t_s} - 1 + e^{B\dot{\varepsilon}_o t} - e^{B\dot{\varepsilon}_o t_s}}{B} \tag{A5b}$$

$$S_3(t) = e^{B\dot{\varepsilon}_s t_s}\left[E_1\left(\frac{\overline{t}}{\tau_2}\right) - E_1\left(\frac{\overline{t}}{\tau_1}\right)\right] + E_1\left(\frac{t}{\tau_1}\right) - E_1\left(\frac{t}{\tau_2}\right) \tag{A5c}$$

$$S_4(t) = e^{B\dot{\varepsilon}_s t}\left[E_1\left(\frac{\overline{t}(1 + B\dot{\varepsilon}_s\tau_1)}{\tau_1}\right) - E_1\left(\frac{\overline{t}(1 + B\dot{\varepsilon}_s\tau_2)}{\tau_2}\right)\right] \tag{A5d}$$

$$S_5(t) = e^{B\dot{\varepsilon}_s t}\left[E_1\left(\frac{t(1 + B\dot{\varepsilon}_s\tau_2)}{\tau_2}\right) - E_1\left(\frac{t(1 + B\dot{\varepsilon}_s\tau_1)}{\tau_1}\right)\right] \tag{A5e}$$

$$S_6(t) = e^{B\dot{\varepsilon}_o t}\left[\ln\left(\frac{1 + B\dot{\varepsilon}_o\tau_2}{1 + B\dot{\varepsilon}_o\tau_1}\right) + E_1\left(\frac{\overline{t}(1 + B\dot{\varepsilon}_o\tau_2)}{\tau_2}\right) - E_1\left(\frac{\overline{t}(1 + B\dot{\varepsilon}_o\tau_1)}{\tau_1}\right)\right] \tag{A5f}$$

$$S_7(t) = e^{B\dot{\varepsilon}_o t_s}\left[E_1\left(\frac{\overline{t}}{\tau_1}\right) - E_1\left(\frac{\overline{t}}{\tau_2}\right)\right] \tag{A5g}$$

$$S_8(t) = \left[E_1\left(\frac{\overline{t}(1 + B\dot{\varepsilon}_s\tau_2)}{\tau_2}\right) - E_1\left(\frac{\overline{t}(1 + B\dot{\varepsilon}_s\tau_1)}{\tau_1}\right)\right] \tag{A5h}$$

$$S_9(t) = \left[E_1\left(\frac{t(1 + B\dot{\varepsilon}_s\tau_1)}{\tau_1}\right) - E_1\left(\frac{t(1 + B\dot{\varepsilon}_s\tau_2)}{\tau_2}\right)\right] \tag{A5i}$$

$$S_{10}(t) = \left[\ln\left(\frac{\tau_2(1 + B\dot{\varepsilon}_o\tau_1)}{\tau_1(1 + B\dot{\varepsilon}_o\tau_2)}\right) + E_1\left(\frac{\overline{t}(1 + B\dot{\varepsilon}_o\tau_{12})}{\tau_1}\right) - E_1\left(\frac{\overline{t}(1 + B\dot{\varepsilon}_o\tau_2)}{\tau_2}\right)\right] \tag{A5j}$$

where

$$\overline{t} = t - t_s \tag{A6}$$

Similarly, the expression for the hold ($t > t_0$) was as follows:

$$F(t) = T_1\left(T_2(t) + \frac{c_1}{B}[T_3(t) + T_4(t) + T_5(t) + T_6(t) + T_7(t) + T_8(t)] + c_2\dot{\varepsilon}_s e^{B\dot{\varepsilon}_s t}[T_9(t) + T_{10}(t)] + c_2\dot{\varepsilon}_o e^{B\dot{\varepsilon}_o t}[T_{11}(t) + T_{12}(t)] \right) \tag{A7}$$

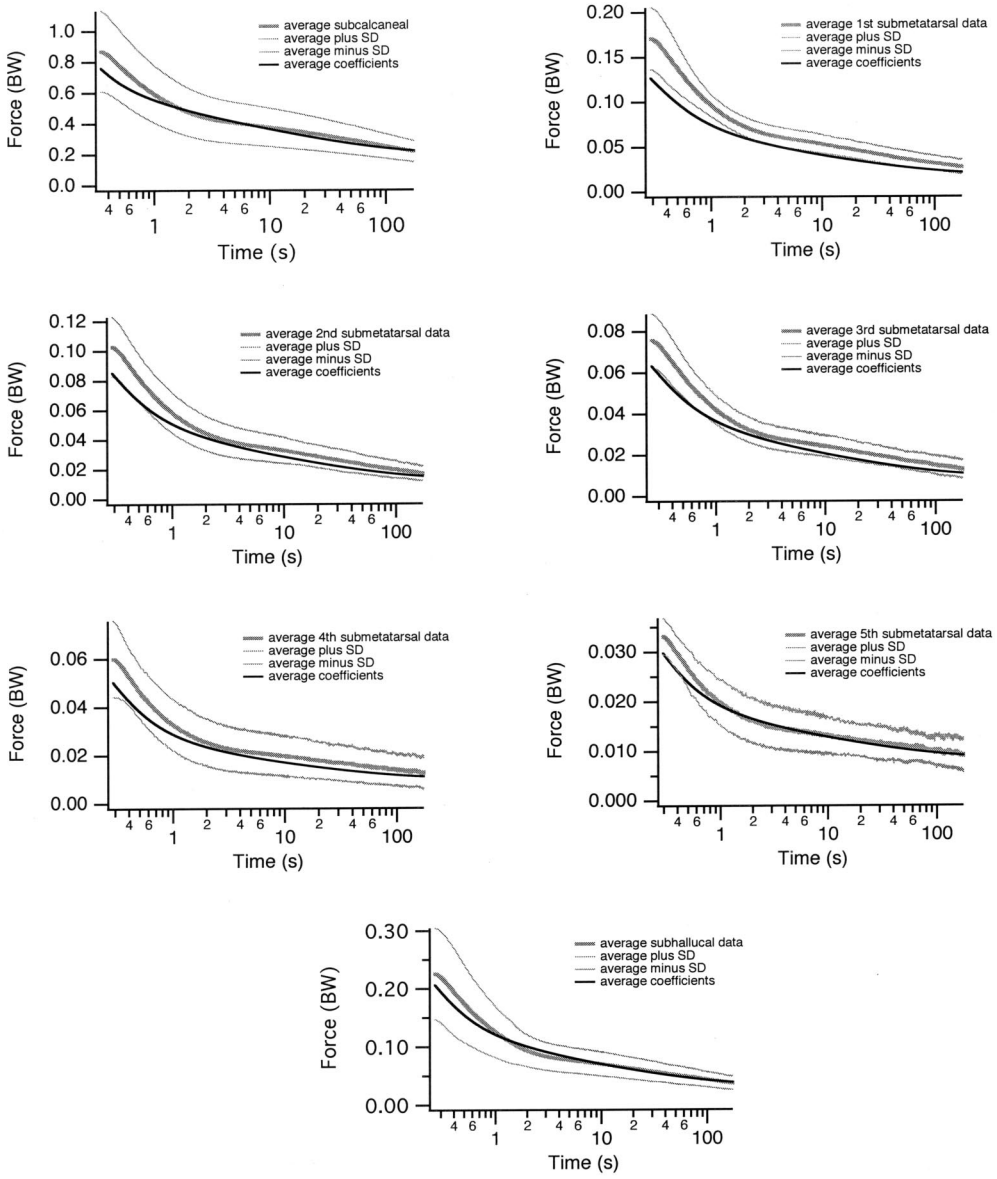

Fig. 3 The average stress relaxation (unnormalized force vs time) data (±1 S.D.) and the fit generated from the average QLV coefficients for the subcalcaneal, five submetarsal, and subhallucal areas. BW=body weight.

$$T_1 = \frac{AB}{1 + c_1 \ln\frac{\tau_2}{\tau_1} + c_2\left(\frac{1}{\tau_1} - \frac{1}{\tau_2}\right)} \tag{A8a}$$

$$T_2(t) = \frac{e^{B\dot{\varepsilon}_s t_s} - 1 + e^{B\dot{\varepsilon}_o t_o} - e^{B\dot{\varepsilon}_o t_s}}{B} \tag{A8b}$$

$$T_3(t) = e^{B\dot{\varepsilon}_s t_s}\left[E_1\left(\frac{\overline{t}}{\tau_2}\right) - E_1\left(\frac{\overline{t}}{\tau_1}\right)\right] + E_1\left(\frac{t}{\tau_1}\right) - E_1\left(\frac{t}{\tau_2}\right) \tag{A8c}$$

$$T_4(t) = e^{B\dot{\varepsilon}_s t}\left[E_1\left(\frac{\overline{t}(1+B\dot{\varepsilon}_s\tau_1)}{\tau_1}\right) - E_1\left(\frac{\overline{t}(1+B\dot{\varepsilon}_s\tau_2)}{\tau_2}\right)\right] \tag{A8d}$$

$$T_5(t) = e^{B\dot{\varepsilon}_s t}\left[E_1\left(\frac{t(1+B\dot{\varepsilon}_s\tau_2)}{\tau_2}\right) - E_1\left(\frac{t(1+B\dot{\varepsilon}_s\tau_1)}{\tau_1}\right)\right] \tag{A8e}$$

$$T_6(t) = e^{B\dot{\varepsilon}_o t_o}\left[E_1\left(\frac{\hat{t}}{\tau_2}\right) - E_1\left(\frac{\hat{t}}{\tau_1}\right)\right] + e^{B\dot{\varepsilon}_o t_s}\left[E_1\left(\frac{\overline{t}}{\tau_1}\right) - E_1\left(\frac{\overline{t}}{\tau_2}\right)\right] \tag{A8f}$$

$$T_7(t) = e^{B\dot{\varepsilon}_s t}\left[E_1\left(\frac{\hat{t}(1+B\dot{\varepsilon}_o\tau_1)}{\tau_1}\right) - E_1\left(\frac{\hat{t}(1+B\dot{\varepsilon}_o\tau_2)}{\tau_2}\right)\right] \tag{A8g}$$

$$T_8(t) = e^{B\dot{\varepsilon}_o t}\left[E_1\left(\frac{\overline{t}(1+B\dot{\varepsilon}_o\tau_2)}{\tau_2}\right) - E_1\left(\frac{\overline{t}(1+B\dot{\varepsilon}_o\tau_1)}{\tau_1}\right)\right] \tag{A8h}$$

$$T_9(t) = \left[E_1\left(\frac{\overline{t}(1+B\dot{\varepsilon}_s\tau_2)}{\tau_2}\right) - E_1\left(\frac{\overline{t}(1+B\dot{\varepsilon}_s\tau_1)}{\tau_1}\right)\right] \tag{A8i}$$

$$T_{10}(t) = \left[E_1\left(\frac{t(1+B\dot{\varepsilon}_s\tau_1)}{\tau_1}\right) - E_1\left(\frac{t(1+B\dot{\varepsilon}_s\tau_2)}{\tau_2}\right)\right] \tag{A8j}$$

$$T_{11}(t)=\left[E_1\left(\frac{\hat{t}(1+B\dot{\varepsilon}_o\tau_2)}{\tau_2}\right)-E_1\left(\frac{\hat{t}(1+B\dot{\varepsilon}_o\tau_1)}{\tau_1}\right)\right] \quad (A8k)$$

$$T_{12}(t)=\left[E_1\left(\frac{\overline{t}(1+B\dot{\varepsilon}_o\tau_1)}{\tau_1}\right)-E_1\left(\frac{\overline{t}(1+B\dot{\varepsilon}_o\tau_2)}{\tau_2}\right)\right] \quad (A8l)$$

where

$$\hat{t}=t-t_o \quad (A9)$$

The general form of the QLV theory, capable of modeling other loading conditions, is derived by substituting Eqs. (3), (4), and (5) into Eq. (1), but without any assumptions made concerning the normalized compression or normalized compression rate [Eq. (*A*10)].

$$\frac{dF}{d\tau'}=\frac{1+c_1E_1\left(\frac{t}{\tau_2}\right)-c_1E_1\left(\frac{t}{\tau_1}\right)+\frac{c_2e^{-t/\tau_2}}{t}-\frac{c_2e^{-t/\tau_1}}{t}}{1+c_1\ln\frac{\tau_2}{\tau_1}+c_2\left(\frac{1}{\tau_1}-\frac{1}{\tau_2}\right)}$$

$$\times ABe^{B\varepsilon(\tau')}\dot{\varepsilon} \quad (A10)$$

References

[1] Sammarco, G. J., 1989, *Biomechanics of the Foot*, Lea & Febiger, Malvern, PA, pp. 163–181.

[2] Sarrafian, S. K., 1993, *Anatomy of the Foot and Ankle: Descriptive, Topographic, Functional*, Lippincott, Philadelphia, PA.

[3] Cavanagh, P. R., Valiant, G. A., et al. (1984). Biological Aspects of Modeling Shoe/Foot Interaction During Running, in *Sports Shoes and Playing Surfaces: Biomechanical Properties*, E. C. Fredericks, Champaign, Illinois, Human Kinetics Publishers, Inc: 24–46.

[4] Kinoshita, H., Ogawa, T., Kuzuhara, K., and Ikuta, K., 1993, ''In Vivo Examination of the Dynamic Properties of the Human Heel Pad.,'' Int. J. Sports Med., **14**(6), pp. 312–319.

[5] Kinoshita, H., Francis, P. R., Murase, T., Kawai, S., and Ogawa, T., 1996, ''The Mechanical Properties of the Heel Pad in Elderly Adults,'' European J. Appl. Physiol. Occup. Physiol., **73**(5), pp. 404–409.

[6] Bennett, M. B., and Ker, R. F., 1990, ''The Mechanical Properties of the Human Subcalcaneal Fat Pad in Compression,'' J. Anat., **171**, pp. 131–138.

[7] Aerts, P., Ker, R. F., De Clercq, D., Ilsley, D. W., and Alexander, R. M., 1995, ''The Mechanical Properties of the Human Heel Pad: A Paradox Resolved,'' J. Biomech., **28**(11), pp. 1299–1308.

[8] Gooding, G. A., Stess, R. M., Graf, P. M., Moss, K. M., Louie, K. S., and Grunfeld, C., 1986, ''Sonography of the Sole of the Foot. Evidence for Loss of Foot Pad Thickness in Diabetes and Its Relationship to Ulceration of the Foot,'' Invest. Radiol., **21**(1), pp. 45–48.

[9] Jahss, M. H., Michelson, J. D., Desai, P., Kaye, R., Kummer, F., Buschman, W., Watkins, F., and Reich, S., 1992, ''Investigations Into the Fat Pads of the Sole of the Foot: Anatomy and Histology,'' Foot Ankle, **13**(5), pp. 233–242.

[10] Phinney, S. D., Stern, J. S., Burke, K. E., Tang, A. B., Miller, G., and Holman, R. T., 1994, ''Human Subcutaneous Adipose Tissue Shows Site-Specific Differences in Fatty Acid Composition,'' Am. J. Clin. Nutr., **60**(5), pp. 725–729.

[11] Buschmann, W. R., Jahss, M. H., Kummer, F., Desai, P., Gee, R. O., and Ricci, J. L., 1995, ''Histology and Histomorphometric Analysis of the Normal and Atrophic Heel Fat Pad,'' Foot Ankle Int., **16**(5), pp. 254–258.

[12] Hsu, T. C., Wang, C. L., Shau, Y. W., Tang, F. T., Li, K. L., and Chen, C. Y., 2000, ''Altered Heel-Pad Mechanical Properties in Patients With Type 2 Diabetes Mellitus,'' Diabetic Med., **17**(12), pp. 854–859.

[13] Miller-Young, J. E., Duncan, N. A., and Baroud, G., 2002, ''Material Properties of the Human Calcaneal Fat Pad in Compression: Experiment and Theory,'' J. Biomech., **35**(12), pp. 1523–1531.

[14] Faure, C., 1981, ''The Skeleton of the Anterior Foot,'' Anat. Clin., **3**, pp. 49–65.

[15] Ledoux, W. R., and Hillstrom, H. J., 2002, ''The Distributed Plantar Vertical Force of Neutrally Aligned and Pes Planus Feet,'' Gait Posture, **15**(1), pp. 1–9.

[16] Fung, Y. C., 1993, *Bioviscoelastic Solids*, Springer, New York, pp. 242–320.

[17] Woo, S. L., Gomez, M. A., and Akeson, W. H., 1981, ''The Time and History-Dependent Viscoelastic Properties of the Canine Medial Collateral Ligament,'' J. Biomech. Eng., **103**(4), pp. 293–298.

[18] Myers, B. S., McElhaney, J. H., and Doherty, B. J., 1991, ''The Viscoelastic Responses of the Human Cervical Spine in Torsion: Experimental Limitations of Quasi-Linear Theory, and a Method for Reducing These Effects,'' J. Biomech., **24**(9), pp. 811–817.

[19] Kwan, M. K., Lin, T. H., and Woo, S. L., 1993, ''On the Viscoelastic Properties of the Anteromedial Bundle of the Anterior Cruciate Ligament,'' J. Biomech., **26**(4–5), pp. 447–452.

[20] Iatridis, J. C., Setton, L. A., Weidenbaum, M., and Mow, V. C., 1997, ''The Viscoelastic Behavior of the Non-Degenerate Human Lumbar Nucleus Pulposus in Shear,'' J. Biomech., **30**(10), pp. 1005–1013.

[21] Funk, J. R., Hall, G. W., Crandall, J. R., and Pilkey, W. D., 2000, ''Linear and Quasi-Linear Viscoelastic Characterization of Ankle Ligaments,'' J. Biomech. Eng., **122**(1), pp. 15–22.

[22] Cavanagh, P. R., 1999, ''Plantar Soft Tissue Thickness During Ground Contact in Walking,'' J. Biomech., **32**(6), pp. 623–628.

[23] Gefen, A., Megido-Ravid, M., and Itzchak, Y., 2001, ''In Vivo Biomechanical Behavior of the Human Heel Pad During the Stance Phase of Gait,'' J. Biomech., **34**(12), pp. 1661–1665.

[24] Sauren, A. A., van Hout, M. C., van Steenhoven, A. A., Veldpaus, F. E., and Janssen, J. D., 1983, ''The Mechanical Properties of Porcine Aortic Valve Tissues,'' J. Biomech., **16**(5), pp. 327–337.

[25] Best, T. M., McElhaney, J., Garrett, Jr., W. E., and Myers, B. S., 1994, ''Characterization of the Passive Responses of Live Skeletal Muscle Using the Quasi-Linear Theory of Viscoelasticity,'' J. Biomech., **27**(4), pp. 413–419.

[26] Galbraith, J. A., Thibault, L. E., and Matteson, D. R., 1993, ''Mechanical and Electrical Responses of the Squid Giant Axon to Simple Elongation,'' J. Biomech. Eng., **115**(1), pp. 13–22.

[27] Wang, C. L., Hsu, T. C., Shau, Y. W., Shieh, J. Y., and Hsu, K. H., 1999, ''Ultrasonographic Measurement of the Mechanical Properties of the Sole Under the Metatarsal Heads,'' J. Orthop. Res., **17**(5), pp. 709–713.

[28] Zheng, Y. P., Choi, Y. K., Wong, K., Chan, S., and Mak, A. F., 2000, ''Biomechanical Assessment of Plantar Foot Tissue in Diabetic Patients Using an Ultrasound Indentation System,'' Ultrasound Med. Biol., **26**(3), pp. 451–456.

[29] Abramowitz, M., and Stegun, A., 1964, *A Handbook of Mathematical Functions*, U.S. Government Printing Office, Washington, D.C.